

VisionReward: Fine-Grained Multi-Dimensional Human Preference Learning for Image and Video Generation

Jiazheng Xu^{1*†}, Yu Huang^{1*†}, Jiale Cheng^{1†}, Yuanming Yang^{1†}, Jiajun Xu^{1†}, Yuan Wang^{1†}, Wenbo Duan^{1†}, Shen Yang^{1†}, Qunlin Jin^{1†}, Shurun Li^{1†}, Jiayan Teng^{1†}, Zhuoyi Yang^{1†}, Wendi Zheng^{1†}, Xiao Liu^{1†}, Dan Zhang^{1†}, Ming Ding², Xiaohan Zhang², Shiyu Huang², Xiaotao Gu², Minlie Huang¹, Jie Tang¹, Yuxiao Dong¹

¹Tsinghua University

²Z.AI

{xjz22, h-y22}@mails.tsinghua.edu.cn, yuxiaod@tsinghua.edu.cn

Abstract

Visual generative models have achieved remarkable progress in synthesizing photorealistic images and videos, yet aligning their outputs with human preferences across critical dimensions remains a persistent challenge. Though reinforcement learning from human feedback offers promise for preference alignment, existing reward models for visual generation face limitations, including black-box scoring without interpretability and potentially resultant unexpected biases. We present VisionReward, a general framework for learning human visual preferences in both image and video generation. Specifically, we employ a hierarchical visual assessment framework to capture fine-grained human preferences, and leverages linear weighting to enable interpretable preference learning. Furthermore, we propose a multi-dimensional consistent strategy when using VisionReward as a reward model during preference optimization for visual generation. Experiments show that VisionReward can significantly outperform existing image and video reward models on both machine metrics and human evaluation. Notably, VisionReward surpasses VideoScore by 17.2% in preference prediction accuracy, and text-to-video models with VisionReward achieve a 31.6% higher pairwise win rate compared to the same models using VideoScore.

Code — <https://github.com/THUDM/VisionReward>

1 Introduction

Visual generative models, including text-to-image (Ding et al. 2021; Ramesh et al. 2021; Saharia et al. 2022; Rombach et al. 2022; Betker et al. 2023; Podell et al. 2023) and text-to-video (Hong et al. 2022; Ho et al. 2022; Villegas et al. 2022; Zheng et al. 2024; Chen et al. 2024a; Yang et al.

*Equal contributions. Core contributors: Jiazheng, Yu, Jiale, Yuanming, Jiajun, Yuan, Wenbo, Shen and Qunlin. Corresponding author: Yuxiao (yuxiaod@tsinghua.edu.cn)

[†]Work done while these authors interned at Z.AI.

Copyright © 2026, Association for the Advancement of Artificial Intelligence (www.aaai.org). All rights reserved.

2024) generation, have recently experienced rapid developments. Through large-scale pretraining, these models can effectively translate textual descriptions into photorealistic images or temporally coherent videos. To further align them with human preferences, reinforcement learning from human feedback (RLHF) (Ouyang et al. 2022)—initially introduced in large language models—has recently been adapted to visual generation tasks (Xu et al. 2023; He et al. 2024).

A key bottleneck in applying RLHF to visual generation lies in developing effective visual reward models. Recent studies (Xu et al. 2023; Kirstain et al. 2023; Wu et al. 2023) have explored training reward models to predict human visual preferences, enabling automatic evaluation and preference optimization for visual generative models. For evaluation, reward models function as automated metrics that quantitatively measure the alignment between generated outputs and human preference criteria (Li et al. 2023). For optimization, reward models identify reliable directions for improving visual generation models. Essentially, they can provide feedback in reinforcement learning or generate preference pairs, thus reducing dependence on human annotation (Black et al. 2023; Fan et al. 2023; Clark et al. 2023).

Despite recent progress in reward models (RMs) for visual generation, two primary challenges remain: First, *lack of interpretability and risk of unexpected bias*. Current RMs for visual generation often suffer from limited interpretability. These models inherently involve complex trade-offs among multiple factors, yet their scoring mechanisms lack transparency regarding how such trade-offs are performed. This opacity raises concerns about *potential unexpected biases*. Though multimodal LLMs like Gemini (Team et al. 2024) and GPT-4o (Achiam et al. 2023) enhance interpretability through explainable rating rationales, their general-purpose architectures usually underperform specialized black-box models in fine-grained assessments (Chen et al. 2024c). This raises a key dilemma: how to design preference prediction method to be interpretable while maintaining accuracy.

a) VisionReward for Text-to-Video Evaluation

Text: A child is eating pizza.



VisionReward (Ours)	
Question: Is smoothness of object's movement good?	
Answer: Yes	Answer: No

Question: Are the details relatively refined?	
Answer: Yes	Answer: No
.....	
Linear Weighted Sum of Binary VQA	
3.71 ✓	> 2.91

VideoScore	
2.76	< 3.33 ✗

b) VisionReward for Text-to-Video Optimization

Text: In a dimly lit, ancient library, Sarah, a young woman with fiery red hair, **pores over an old book, whispering an incantation.**



Original



DPO with VideoScore



DPO with VisionReward (Ours)

Figure 1: Illustration of how VisionReward works for evaluation and optimization of visual generation. a) **Evaluation**: VisionReward performs comprehensive evaluation through dimension-specific binary visual QA testing, producing human-aligned, fine-grained assessment scores. b) **Optimization**: VisionReward enable better preference optimization, enhancing multiple key aspects.

Second, *lack of effective reward models for video generation*. The rapid development of text-to-video generative models has intensified the demand for video reward models. Although image reward models can assess individual frame quality, their frame-level nature inherently neglects essential temporal dependencies in video sequences. While VideoScore (He et al. 2024) has pioneered direct video evaluation through learnable metrics, it still suffers from limitations such as insufficient accuracy in preference prediction and optimization in video generation.

Contribution. To address these challenges, we propose a general framework VisionReward to build accurate reward models for both image and video generation. VisionReward is trained with two steps: *fine-grained visual assessment* and *interpretable preference learning*. First, to capture human visual preferences, we identify nine major dimensions and decouple preferences into 64 fine-grained questions. Second, to ensure interpretable preference learning, we propose to use the classical linear weighting mechanism on the question outcomes. It enables intuitive visualization of each question’s impact.

To apply it as a reward model for visual generation models, we propose a *multi-dimensional consistent strategy* during preference optimization. The goal of this strategy is to mitigate unintended and unquantifiable biases. Specifically, a pair of visual samples is used for preference optimization (e.g., DPO (Wallace et al. 2024)) only if one sample is consistently preferred over the other across all dimensions.

To summarize, we present VisionReward as a general

framework for visual preference learning. Empirically, we show that VisionReward makes the following contributions:

- We design fine-grained multi-dimensional preference annotation and build the most fine-grained dataset which contain 81K samples and 5M binary annotation, which enable the training of VisionReward.
- For visual preference prediction, VisionReward achieves state-of-the-art performance across multiple benchmarks, while maintaining interpretability via hierarchical diagnostic QA and explicit linear weighting. For instance, VisionReward outperforms VideoScore (He et al. 2024) by 17.2% in accuracy on preference prediction.
- For visual generation, VisionReward can serve as an effective reward model for preference optimization (e.g., DPO), significantly enhancing the text-to-image and text-to-video models. For example, video generation models with VisionReward achieve a 31.6% higher pairwise win rate compared to the same models using VideoScore.

2 Related Work

Reinforcement Learning from Human Feedback (RLHF) (Stienon et al. 2020; Nakano et al. 2021; Ouyang et al. 2022) refers to optimizing models with reinforcement learning based on human feedback, which is also explored in image and video generation.

Preference Learning for Visual Generation. There are many works learning from human preferences, which collect human annotation for text-to-image (Xu et al. 2023; Kirstain

Dataset	Image	Video	#Samples	#Dimensions	#Fine-Grained	#Annotation
ImageReward (Xu et al. 2023)	✓		9K	-	-	0.1M
Pick-a-Pic (Kirstain et al. 2023)	✓		38K	-	-	0.6M
HPDv2 (Wu et al. 2023)	✓		430K	-	-	0.8M
RichHF-18K (Liang et al. 2024)	✓		18K	4	-	0.1M
MPS (Zhang et al. 2024b)	✓		608K	4	-	2.4M
VideoScore (He et al. 2024)		✓	38K	5	-	0.2M
VisionReward (Ours)	✓	✓	81K	18–20	61–64	5.0M

Table 1: Comparison of dataset of VisionReward and other datasets.

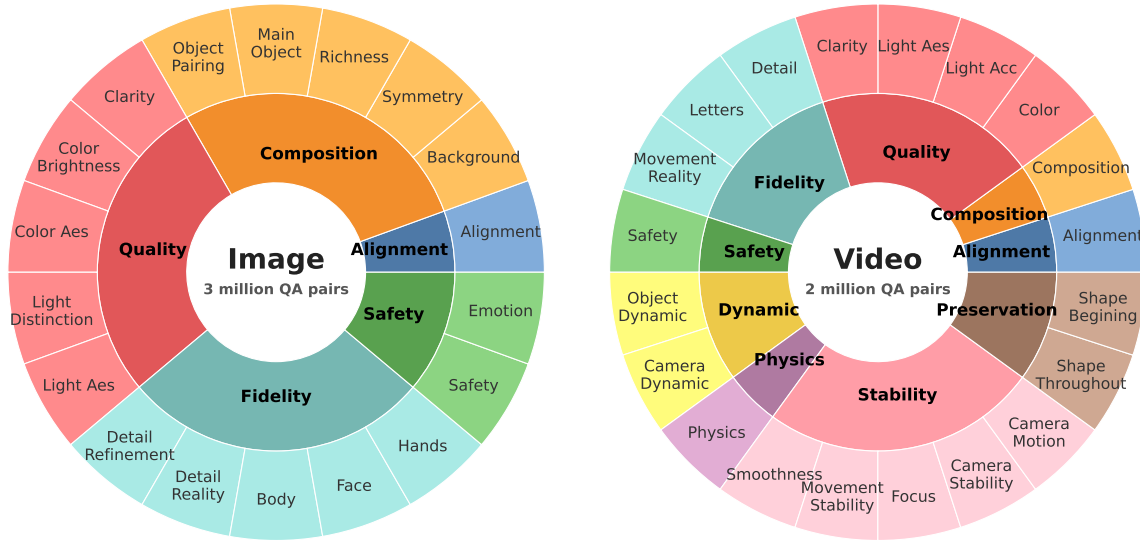


Figure 2: Illustration of fine-grained multi-dimensional design. (Left) For image: 5 dimensions, 18 sub-dimensions, and 61 binary questions. (Right) For video: 9 dimensions, 20 sub-dimensions, and 64 binary questions.

et al. 2023; Wu et al. 2023) and text-to-video (He et al. 2024). Note that existing approaches (Zhang et al. 2024b; Liang et al. 2024) have attempted to augment human annotations or expand dimensions of human preferences in visual generation. Different from them, VisionReward defines fine-grained multi-dimensional human preferences with the goal of disentangling distinct factors to decouple human preferences, to build more accurate and interpretable RM.

RLHF for Visual Generation. For visual generation tasks, several works have explored RLHF, optimizing from the gradient (Xu et al. 2023; Wu et al. 2024) or using a policy-based RL approach (Black et al. 2023; Fan et al. 2023; Clark et al. 2023). All these methods require a reward model (RM) to provide feedback for online learning. Diffusion-DPO (Wallace et al. 2024) has proposed to optimize the diffusion model directly using human-labeled preference data. However, most RLHF methods face the issue of biased-optimization. By employing a multi-dimensional method, VisionReward achieves robust RLHF.

Preliminary for Diffusion-DPO. Given a data distribution $q(x_0)$, Diffusion models (Sohl-Dickstein et al. 2015; Ho, Jain, and Abbeel 2020; Song et al. 2020) contains

forward process and reverse process. Forward process $q(x_{1:T}|x_0)$ gradually add noise to the data x_0 and reverse process $p_\theta(x_{0:T})$ learns transitions to recover data. Training diffusion model can be performed by evidence lower bound (Kingma et al. 2021; Song et al. 2021):

$$L_{\text{DM}} = \mathbb{E}_{\mathbf{x}_0, \epsilon \sim \mathcal{N}(0, \mathbf{I}), t} \left[\|\epsilon - \epsilon_\theta(\mathbf{x}_t, t)\|_2^2 \right], \quad (1)$$

with $t \sim \mathcal{U}(0, T)$ and $\mathbf{x}_t \sim q(\mathbf{x}_t | \mathbf{x}_0)$.

Diffusion-DPO (Wallace et al. 2024) introduces direct preference optimization based on preference pairs. We denote the “win” and “lose” samples as x_0^w, x_0^l , and the objective is as follows:

$$\begin{aligned} \mathcal{L}(\theta) = & -\mathbb{E}_{t \sim \mathcal{U}(0, T), \mathbf{x}_t^w \sim q(\mathbf{x}_t^w | \mathbf{x}_0^w), \mathbf{x}_t^l \sim q(\mathbf{x}_t^l | \mathbf{x}_0^l)} \\ & \log \sigma(-\beta T \omega(\lambda_t) (\\ & \|\epsilon^w - \epsilon_\theta(\mathbf{x}_t^w, t)\|_2^2 - \|\epsilon^w - \epsilon_{\text{ref}}(\mathbf{x}_t^w, t)\|_2^2 \\ & - (\|\epsilon^l - \epsilon_\theta(\mathbf{x}_t^l, t)\|_2^2 - \|\epsilon^l - \epsilon_{\text{ref}}(\mathbf{x}_t^l, t)\|_2^2))) \end{aligned} \quad (2)$$

DPO is ordinarily based on overall preference, which may be biased. VisionReward enables Multi-Dimensional Preference Optimization to enhance it.

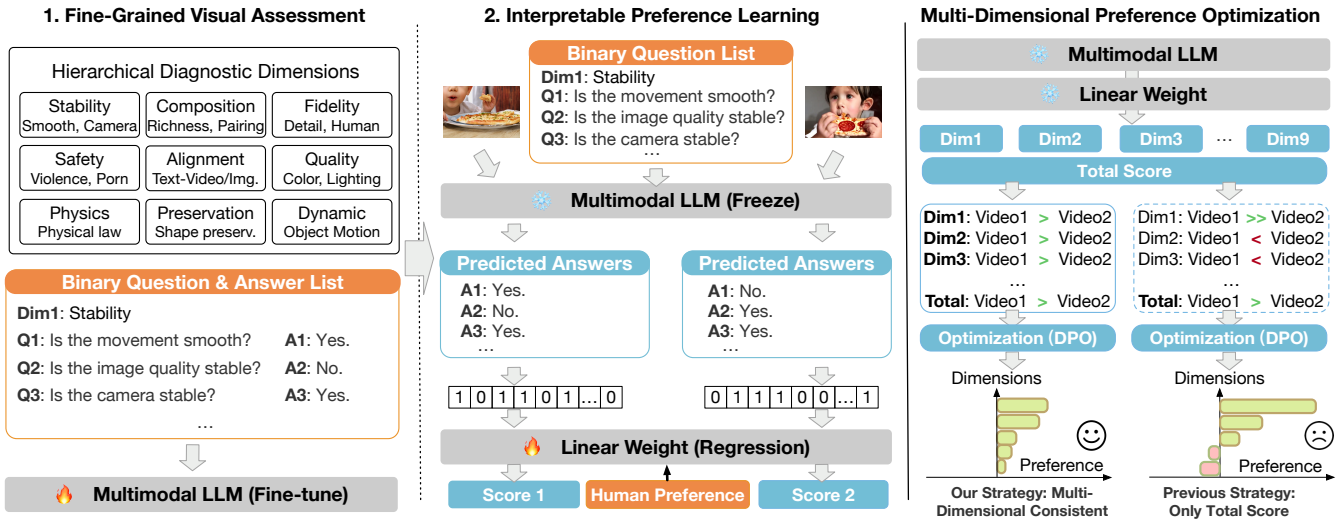


Figure 3: Overall framework of VisionReward. 1) Fine-grained Visual Assessment: fine-tune multimodal LLM to perform binary visual question-answering through hierarchical dimensions. 2) Interpretable Preference Learning: utilize visual QA outputs to predict preferences through linear weighted summation. 3) Multi-Dimensional Preference Optimization: optimization strategy across multiple dimensions.

3 VisionReward

3.1 VisionReward Annotation

Fine-Grained Design. Human preferences are often a result of the interplay of multiple factors (Palmer, Schloss, and Sammartino 2013; Ibarra et al. 2017), necessitating a balance among various considerations. To deconstruct human preferences systematically, we develop a fine-grained multi-dimensional framework, as shown in Table 1 and Fig. 2. For each sub-dimension, we set options that vary gradually in degree, and decompose these options into a series of binary questions (Cf. Tables 15 to 18 in Appendix).

Dataset Preparation. For images, we sample images from multiple popular datasets, including ImageRewardDB (Xu et al. 2023), HPDv2 (Wu et al. 2023), and Pick-a-Pic (Kirstain et al. 2023), and obtain 48k images after filtering. For videos, we sample prompts from Vid-ProM (Wang and Yang 2024). To ensure diversity of prompts, we use Rouge-L (Lin 2004) for initial filtering, follow UniFL (Zhang et al. 2024a) to perform a semantic-based filtering, and use ChatGPT (Achiam et al. 2023) for data cleaning, finally get 10k prompts. Then we use CogVideoX (Yang et al. 2024), VideoCrafter2 (Chen et al. 2024a) and OpenSora (Zheng et al. 2024) to generate 30k videos, sample from Panda-70M (Chen et al. 2024b) to get 3k real videos, leading to 33k videos for annotation. More details are provided in Appendix Section 6.1.

Annotation Management. To avoid bias of annotators, our annotation management includes professional management and standard document. Cooperating with a specialized company, we strictly conduct annotation training for annotators, select qualified annotators, and perform quality inspection of annotation results. Our annotation document

gives clear definitions and provides more than 10 examples for each judgment, to align the standard among annotators. Due to these efforts, the consistency of annotators in the binary results reaches **89.29%** (images) and **89.33%** (videos).

Annotation Analysis. Through specialized annotation, we obtain an image dataset containing 48k images and **3 million** question-answer pairs, while a video dataset with 33k videos and **2 million** pairs. More statistical analysis of the annotation results is in Appendix Section 6.2.

3.2 VisionReward Training

The complete training process of VisionReward and its application methodology during preference optimization are illustrated in Fig. 3.

Fine-grained Visual Assessment. Specifically, we use CogVLM2 (Hong et al. 2024b) as the base model for image understanding, and CogVLM2-Video (Hong et al. 2024b) as the base model for video understanding. In terms of data, we have obtained millions of annotated binary question-answering pairs. Initially, we performed a balanced sampling on each binary question by addressing the imbalance between positive and negative examples, ensuring a roughly equal number of positive and negative instances associated with each binary question. Then we use balanced instruction tuning dataset consisting of binary questions to fine-tune base VLM.

Interpretable Preference Learning. After trained on fine-grained dataset, VisionReward can be adopt to give a series of binary response answers (“yes” or “no”) $\{A_i\}_{i=1}^N$, where N represents the number of binary questions. We define reward of every binary question as $\{x_i\}_{i=1}^N$:

$$x_i = \mathbb{1}[A_i = \text{“yes”}]. \tag{3}$$

We construct a feature vector $X = (x_1, \dots, x_N)$, and use a set of linear weights $W = (w_1, \dots, w_N)$ to obtain the final reward R :

$$R = \sum_{i=1}^N w_i \mathbb{1}[A_i = \text{“yes”}]. \quad (4)$$

In order to learn linear weights W , we collect human preferences for pairs of $\{(X_i, X_j)\}$. Specifically, we compute the feature difference for each pair, given by $\Delta X = X_i - X_j$, and the corresponding label is assigned as $y = 1$ or $y = 0$ depending on the human preference. We then perform logistic regression $y = \Delta X W^T$ to learn linear weights W :

$$\mathcal{L}(W) = -\mathbb{E} [y \log(\sigma(\Delta X W^T)) + (1 - y) \log(1 - \sigma(\Delta X W^T))]. \quad (5)$$

By calculating dimension-specific scores through intra-dimensional weighting, VisionReward facilitates multi-dimensional preference prediction. We note dimensions as $\{\text{dim}_k\}_{k=1}^K$ where dim_k contains questions belonging to the dimension. Then we define reward for certain dimension as:

$$R(\text{dim}_k) = \sum_{i \in \text{dim}_k} w_i \mathbb{1}[A_i = \text{“yes”}]. \quad (6)$$

3.3 Multi-Dimensional Preference Optimization

To empirically validate the model’s capacity, we leverage Direct Preference Optimization (DPO) (Wallace et al. 2024) for Diffusion Models in our experiments, where VisionReward generates multi-dimensional preference pairs to guide the optimization process while maintaining inter-dimensional balance.

Challenges. We replicate the Diffusion-DPO training procedure using SDXL (Podell et al. 2023) on the Pick-a-Pic (Kirstain et al. 2023) dataset, employing VisionReward for comprehensive data analysis and model evaluation. As demonstrated in Fig. 4, both the preference data and optimized model exhibit biases across several fine-grained dimensions. These findings not only underscore VisionReward’s capability for fine-grained analysis but also emphasize the necessity for optimization approaches that account for multi-dimensional representation.

MPO: Insight and Solution. Compared to ordinary DPO method which select pairs using overall preference, we propose MPO-enhanced DPO that take account fine-grained multi-dimensional preference. For reward of two samples R^i and R^j , we define R^i as dominating R^j if $R^i(\text{dim}_k) \geq R^j(\text{dim}_k)$ holds for every dimension dim_k . The key differences between the MPO strategy and standard DPO are:

- **Ordinary DPO:** During DPO optimization, we directly select the pair based on the total reward R .
- **MPO-enhanced DPO:** MPO strategy introduces an additional constraint: we only select pairs that R^i dominates R^j , then proceed with standard DPO.

We analyze the effects of MPO in Section 4.3. The MPO strategy can also be applied to other algorithms, which we leave for future exploration.

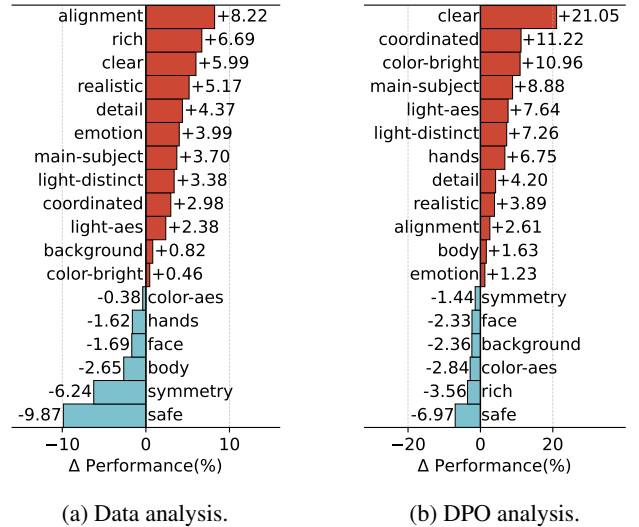


Figure 4: (a) We sample 10,000 human preference pairs from Pick-a-Pic dataset and analyze score deviations across 18 sub-dimensions (represented by the average yes-proportion of checklist questions within each sub-dimension). (b) We show score deviations for images generated by SDXL after Diffusion-DPO, using the same 10,000 prompts.

4 Experiments

4.1 VisionReward for Text-to-Vision Evaluation

Dataset & Training Setting. After balanced sampling, we obtain 40,743 images and corresponding 97,680 judgment questions for training, leaving 6,910 images for subsequent validation and test. For videos, we obtain 28,605 videos and corresponding 89,473 judgment questions for training, with 3,080 videos reserved.

To fine-tune CogVLM2 (Hong et al. 2024b), we set a batch size of 64, a learning rate of 1e-6, and train for 1,500 steps. For CogVLM-Video, we set a batch size of 64, a learning rate of 4e-6, and train for 1,500 steps.

To learn linear weights for preference prediction, we sample human preference pairs and perform logistic regression. For images, We sample 44k pairs (24k from HPDv2 (Wu et al. 2023) and 20k from ImageRewardDB (Xu et al. 2023)); and for videos, we sample prompts from VidProM (Wang and Yang 2024) and generate videos (using CogVideoX (Yang et al. 2024), VideoCrafter2 (Chen et al. 2024a) and OpenSora (Zheng et al. 2024)), getting 1,795 annotated video pairs with preference.

To establish a comprehensive evaluation benchmark for both image and video generation, we construct **MonetBench**, which contains separate test sets for images and videos, each consisting of 1,000 prompts. More details are introduced in Appendix Section 12.

Main Results: Preference Accuracy. Preference accuracy means the probability that a reward model has the same judgment as humans about which image is better. We use MonetBench to construct our test set for human preference,

Method	Image			Video			
	HPDv2	MonetBench		GenAI-Bench		MonetBench	
		tau*	diff**	tau	diff	tau	diff
<i>task-specific discriminative models</i>							
ImageReward (Xu et al. 2023)	74.0	48.8	56.5	48.4	72.1	55.8	58.4
PickScore (Kirstain et al. 2023)	79.8	49.8	57.6	<u>52.4</u>	<u>75.4</u>	57.7	61.6
HPSv2 (Wu et al. 2023)	83.3	48.4	55.6	49.3	73.0	59.3	62.5
MPS (Zhang et al. 2024b)	<u>83.5</u>	44.2	50.7	46.9	67.6	55.8	58.9
<i>generative models</i>							
GPT-4o (Achiam et al. 2023)	77.5	38.9	52.7	41.8	54.3	45.7	48.3
Gemini (Team et al. 2024)	60.7	27.4	55.1	46.9	61.7	52.2	56.8
VQAScore (Lin et al. 2025)	69.7	49.4	56.5	45.2	68.0	56.1	59.5
VideoScore (He et al. 2024)	76.8	45.8	52.5	47.8	71.4	49.1	54.9
VisionReward (Ours)	81.7	51.8	59.5	51.8	74.4	64.0	72.1

Table 2: Preference accuracy on multiple dataset. **Bold** denotes the best score within the generative models, while underline signifies the best score among all categories. Tau* means taking account of ties (Deutsch, Foster, and Freitag 2023), and diff** means dropping ties in labels (we drop ties both in labels and responses for GPT-4o and Gemini in diff** because too many ties are given by them).

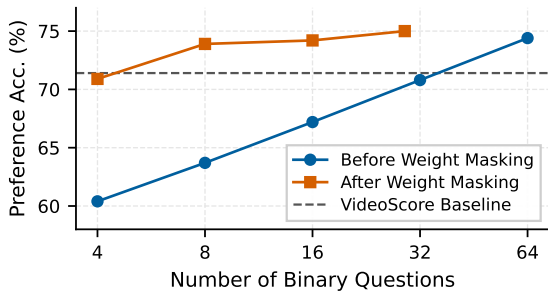


Figure 5: The accuracy of VisionReward on GenAI-Bench improves as the number of binary questions increases. After masking weights from full regression, VisionReward maintains high performance.

using SDXL (Podell et al. 2023) to generate images and CogVideoX (Yang et al. 2024) / VideoCrafter2 (Chen et al. 2024a) / OpenSora (Zheng et al. 2024) to generate videos, resulting in 500 pairs for image and 1,000 pairs for video. We employ annotators to assess the generated images using a preference rating scale from 1 to 5 (with 3 indicating no preference). The average preference score is used as the final preference label. We also take HPDv2 (Wu et al. 2023) and GenAI-Bench (Jiang et al. 2024) as test set.

Table 2 shows that VisionReward obtains state-of-the-state results in multiple datasets. Notably, in video evaluation, image reward models demonstrate competitive performance when the video duration is within 2 seconds (GenAI-Bench). However, when **the video duration reaches 6 seconds (MonetBench)**, only VisionReward is capable of accurately predicting human preference, being twice (**22.1% over random**) as high as the best (12.5% over random) among other methods. This indicates that dynamic information in longer videos poses a challenge for RMs, while

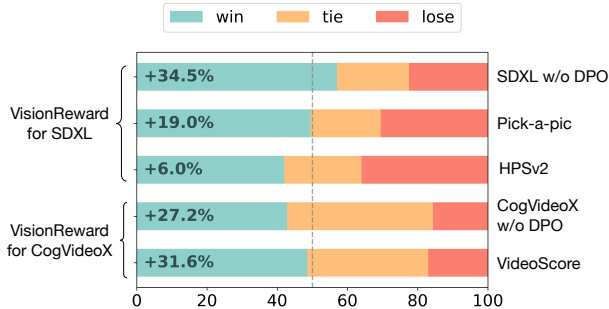


Figure 6: Human evaluation results of DPO using different reward models or preference datasets. We require five annotators to comprehensively evaluate two samples and select the better one. VisionReward achieve the best performance.

VisionReward can effectively address this issue after fine-grained visual learning.

Ablation Study: Scalability of Question Scale. Fig. 5 shows that accuracy of preference prediction exhibits significant improvement as the question scale increases, and masking minimal weights maintains performance (Details in Appendix Section 7). Scalability validates the effects of decomposing preferences via fine-grained questions. We do more analysis of VisionReward in Appendix Section 7 and analysis of fine-grained results in Section 10.

4.2 VisionReward for Preference Optimization

To evaluate the efficacy of VisionReward in preference optimization for visual generative systems, we conduct a series of comparative experiments against current state-of-the-art reward models and established preference datasets. We use SDXL as text-to-image base model and CogVideoX as text-to-video base model. The empirical results presented in Fig. 6 demonstrate VisionReward’s superior performance,

achieving statistically significant improvements in human preference metrics over competing approaches.

This section focuses on preference optimization for text-to-video using different reward models. Details of text-to-image are provided in Appendix Section 8.2.

Dataset & Training Settings. For our backbone model, we select CogVideoX-2B. The training prompts are sampled from VidProM (Wang and Yang 2024) (details in Appendix Section 8.1). To adapt these prompts for video generation, we have optimized them following guidelines from CogVideoX (Yang et al. 2024), which results in roughly 22,000 samples. We generate 4 videos for each prompt, and use VisionReward to score these videos and apply the MPO strategy to select approximately 9,400 effective preference pairs. In all our experiments, we maintain a batch size of 32, a learning rate of $5e-6$, and employ 100 warmup steps followed by linear decay. We set the DPO parameter β to 500. The MPO training process spans around 500 steps, equivalent to about 2 epochs. During training, we save a checkpoint every 40 steps and use a validation set split from the training set to pick the checkpoint with the highest reward.

Evaluation Settings. To comprehensively assess the MPO models, we have conducted both automatic and human evaluations. The automatic evaluation is conducted across various benchmarks, including VBench (Huang et al. 2024) and our Video-MonetBench. For VBench, we focus on commonly reported key metrics, including *Human Action*, *Scene*, *Multiple Objects*, and *Appearance Style*. In all these experiments, we utilize prompt optimization recommended in CogVideoX. Our baseline comparisons include the original CogVideoX-2B and DPO with VideoScore.

Methods	Human Action	Scene	Multiple Objects	Appear. Style
Original	98.20	55.60	68.43	24.20
VideoScore	97.60	56.25	68.66	23.96
VisionReward	98.40	57.57	71.54	24.02

Table 3: Evaluation results on VBench.

Experimental Results. The main results are shown in Table 3. When compared to the original CogVideoX-2B, optimization with VisionReward significantly enhances model performance across these benchmarks. In contrast, optimization with VideoScore tends to degrade performance. The empirical evidence substantiates VisionReward’s advanced capacity for multi-dimensional optimization. (Case study in Appendix Section 8.3.)

4.3 Ablation Study of MPO

To comprehensively illustrate how MPO addresses the factor optimization bias inherent in DPO, We conduct experiments based on CogVideoX-5B. We set the threshold of the total score to 0.8 for DPO and 0.6 for MPO, ensuring that the number of pairs obtained through all three strategies is 5k. We use a batch size of 64, a learning rate of $2e-6$, the DPO parameter β of 500, and the training steps of

300. VisionReward is employed to evaluate scores across various dimensions, with the detailed results presented in Table 4. Through the implementation of the MPO strategy, CogVideoX is optimized in such a manner that it avoids the degradation of certain factors (e.g., alignment), thereby achieving improved trade-offs, such as maintaining good preservation while avoiding excessively slow dynamic changes. The empirical evidence further substantiates VisionReward’s capacity for algorithm-agnostic preference alignment, as evidenced by comparative testing with other approaches like MaPO (Hong et al. 2024a).

Method	Align.	Quality	Dynamic	Physics	Preserv.	Overall
Original	1.733	0.660	0.053	0.344	0.653	4.303
DPO	1.697	0.680	0.034	0.356	0.741	4.515
DPO w/ MPO	1.766	0.688	0.042	0.356	0.721	4.573
MaPO	1.736	0.660	0.052	0.345	0.645	4.295
MaPO w/ MPO	1.737	0.656	0.055	0.349	0.649	4.321

Table 4: Ablation Study of MPO strategy. Scores are given by VisionReward on MonetBench.

For efficiency discussion, the experimental results in Table 5 reveal the comparative effectiveness of the MPO and DPO methods. We analyze the pairs selected in perspective of “ R^i dominating R^j ” mentioned in Section 3.3. These results suggest that MPO outperforms the DPO approach in terms of both efficiency and effectiveness. These findings highlight promising directions for future research in developing novel optimization algorithms and adapting VisionReward for multi-dimensional optimization.

Method	#Dom.	#Not-Dom.	Reward
Original	-	-	4.303
DPO w/o MPO	3814	1456	4.515 (+0.212)
DPO w/ MPO	5028	0	4.573 (+0.270)
Δ (vs w/o MPO)	+31.8%	-100%	+27.4%

Table 5: Comparison of MPO and DPO on MonetBench. “#Dom.” means the number of pairs that match the rule of “ R^i dominating R^j ”, while “#Not-Dom.” pairs not match.

5 Conclusion

We introduce VisionReward, a reward model for visual generation, which is fine-grained and multi-dimensional. By enabling Vision-Language Model (VLM) to perform binary assessments and applying linear summation with weighting coefficients derived from preference learning, VisionReward achieves highly accurate and interpretable. For visual generative optimization, VisionReward surpasses other reward models and enable multi-dimensional strategy.

Acknowledgments

This research was supported by Natural Science Foundation of China (NSFC) No. 62276148, NSFC No. 62495063. The authors would like to thank Z.AI for sponsoring the computation resources used in this work.

References

- Achiam, J.; Adler, S.; Agarwal, S.; Ahmad, L.; Akkaya, I.; Aleman, F. L.; Almeida, D.; Altenschmidt, J.; Altman, S.; Anadkat, S.; et al. 2023. Gpt-4 technical report. *arXiv preprint arXiv:2303.08774*.
- Betker, J.; Goh, G.; Jing, L.; Brooks, T.; Wang, J.; Li, L.; Ouyang, L.; Zhuang, J.; Lee, J.; et al. 2023. Improving image generation with better captions. *Computer Science*. <https://cdn.openai.com/papers/dall-e-3.pdf>, 2(3): 8.
- Black, K.; Janner, M.; Du, Y.; Kostrikov, I.; and Levine, S. 2023. Training diffusion models with reinforcement learning. *arXiv preprint arXiv:2305.13301*.
- Chen, H.; Zhang, Y.; Cun, X.; Xia, M.; Wang, X.; Weng, C.; and Shan, Y. 2024a. Videocrafter2: Overcoming data limitations for high-quality video diffusion models. In *Proceedings of the IEEE/CVF Conference on Computer Vision and Pattern Recognition*, 7310–7320.
- Chen, T.-S.; Siarohin, A.; Menapace, W.; Deyneka, E.; Chao, H.-w.; Jeon, B. E.; Fang, Y.; Lee, H.-Y.; Ren, J.; Yang, M.-H.; et al. 2024b. Panda-70m: Captioning 70m videos with multiple cross-modality teachers. In *Proceedings of the IEEE/CVF Conference on Computer Vision and Pattern Recognition*, 13320–13331.
- Chen, Z.; Du, Y.; Wen, Z.; Zhou, Y.; Cui, C.; Weng, Z.; Tu, H.; Wang, C.; Tong, Z.; Huang, Q.; et al. 2024c. MJ-Bench: Is Your Multimodal Reward Model Really a Good Judge for Text-to-Image Generation? *arXiv preprint arXiv:2407.04842*.
- Clark, K.; Vicol, P.; Swersky, K.; and Fleet, D. J. 2023. Directly fine-tuning diffusion models on differentiable rewards. *arXiv preprint arXiv:2309.17400*.
- Deutsch, D.; Foster, G.; and Freitag, M. 2023. Ties Matter: Meta-Evaluating Modern Metrics with Pairwise Accuracy and Tie Calibration. In *Proceedings of the 2023 Conference on Empirical Methods in Natural Language Processing*, 12914–12929.
- Ding, M.; Yang, Z.; Hong, W.; Zheng, W.; Zhou, C.; Yin, D.; Lin, J.; Zou, X.; Shao, Z.; Yang, H.; et al. 2021. Cogview: Mastering text-to-image generation via transformers. *Advances in Neural Information Processing Systems*, 34: 19822–19835.
- Fan, Y.; Watkins, O.; Du, Y.; Liu, H.; Ryu, M.; Boutilier, C.; Abbeel, P.; Ghavamzadeh, M.; Lee, K.; and Lee, K. 2023. DPoK: reinforcement learning for fine-tuning text-to-image diffusion models. In *Proceedings of the 37th International Conference on Neural Information Processing Systems*, 79858–79885.
- GLM, T. 2024. ChatGLM: A Family of Large Language Models from GLM-130B to GLM-4 All Tools. *arXiv:2406.12793*.
- He, X.; Jiang, D.; Zhang, G.; Ku, M.; Soni, A.; Siu, S.; Chen, H.; Chandra, A.; Jiang, Z.; Arulraj, A.; et al. 2024. VideoScore: Building Automatic Metrics to Simulate Fine-grained Human Feedback for Video Generation. In *Proceedings of the 2024 Conference on Empirical Methods in Natural Language Processing*, 2105–2123.
- Ho, J.; Chan, W.; Saharia, C.; Whang, J.; Gao, R.; Gritsenko, A.; et al. 2022. Imagen video: High definition video generation with diffusion models. *arXiv preprint arXiv:2210.02303*.
- Ho, J.; Jain, A.; and Abbeel, P. 2020. Denoising diffusion probabilistic models. *Advances in neural information processing systems*, 33: 6840–6851.
- Hong, J.; Paul, S.; Lee, N.; Rasul, K.; Thorne, J.; and Jeong, J. 2024a. Margin-aware preference optimization for alignment diffusion models without reference. *arXiv preprint arXiv:2406.06424*.
- Hong, W.; Ding, M.; Zheng, W.; Liu, X.; and Tang, J. 2022. Cogvideo: Large-scale pretraining for text-to-video generation via transformers. *arXiv preprint arXiv:2205.15868*.
- Hong, W.; Wang, W.; Ding, M.; Yu, W.; Lv, Q.; Wang, Y.; Cheng, Y.; Huang, S.; Ji, J.; Xue, Z.; et al. 2024b. CogVLM2: Visual language models for image and video understanding. *arXiv preprint arXiv:2408.16500*.
- Huang, Z.; He, Y.; Yu, J.; Zhang, F.; Si, C.; Jiang, Y.; Zhang, Y.; Wu, T.; Jin, Q.; Chanpaisit, N.; et al. 2024. Vbench: Comprehensive benchmark suite for video generative models. In *Proceedings of the IEEE/CVF Conference on Computer Vision and Pattern Recognition*, 21807–21818.
- Ibarra, F. F.; Kardan, O.; Hunter, M. R.; Kotabe, H. P.; Meyer, F. A.; and Berman, M. G. 2017. Image feature types and their predictions of aesthetic preference and naturalness. *Frontiers in Psychology*, 8: 632.
- Jiang, D.; Ku, M.; Li, T.; Ni, Y.; Sun, S.; Fan, R.; and Chen, W. 2024. GenAI Arena: An Open Evaluation Platform for Generative Models. *arXiv preprint arXiv:2406.04485*.
- Kingma, D.; Salimans, T.; Poole, B.; and Ho, J. 2021. Variational diffusion models. *Advances in neural information processing systems*, 34: 21696–21707.
- Kirstain, Y.; Polyak, A.; Singer, U.; Matiana, S.; Penna, J.; and Levy, O. 2023. Pick-a-pic: An open dataset of user preferences for text-to-image generation. *Advances in Neural Information Processing Systems*, 36: 36652–36663.
- Li, C.; Zhang, Z.; Wu, H.; Sun, W.; Min, X.; Liu, X.; Zhai, G.; and Lin, W. 2023. Agiqa-3k: An open database for ai-generated image quality assessment. *IEEE Transactions on Circuits and Systems for Video Technology*, 34(8): 6833–6846.
- Li, F.; Zhang, R.; Zhang, H.; Zhang, Y.; Li, B.; Li, W.; Ma, Z.; and Li, C. 2024. Llava-next-interleave: Tackling multi-image, video, and 3d in large multimodal models. *arXiv preprint arXiv:2407.07895*.
- Liang, Y.; He, J.; Li, G.; Li, P.; Klimovskiy, A.; Carolan, N.; Sun, J.; Pont-Tuset, J.; Young, S.; Yang, F.; et al. 2024. Rich human feedback for text-to-image generation. In *Proceedings of the IEEE/CVF Conference on Computer Vision and Pattern Recognition*, 19401–19411.
- Lin, C.-Y. 2004. ROUGE: A Package for Automatic Evaluation of Summaries. In *Text Summarization Branches Out*, 74–81. Barcelona, Spain: Association for Computational Linguistics.

- Lin, Z.; Pathak, D.; Li, B.; Li, J.; Xia, X.; Neubig, G.; Zhang, P.; and Ramanan, D. 2025. Evaluating text-to-visual generation with image-to-text generation. In *European Conference on Computer Vision*, 366–384. Springer.
- Liu, H.; Li, C.; Wu, Q.; and Lee, Y. J. 2023. Visual Instruction Tuning.
- Nakano, R.; Hilton, J.; Balaji, S.; Wu, J.; Ouyang, L.; et al. 2021. Webgpt: Browser-assisted question-answering with human feedback. *arXiv preprint arXiv:2112.09332*.
- Ouyang, L.; Wu, J.; Jiang, X.; Almeida, D.; Wainwright, C.; Mishkin, P.; Zhang, C.; Agarwal, S.; Slama, K.; Ray, A.; et al. 2022. Training language models to follow instructions with human feedback. *Advances in Neural Information Processing Systems*, 35: 27730–27744.
- Palmer, S. E.; Schloss, K. B.; and Sammartino, J. 2013. Visual aesthetics and human preference. *Annual review of psychology*, 64(1): 77–107.
- Podell, D.; English, Z.; Lacey, K.; Blattmann, A.; Dockhorn, T.; Müller, J.; Penna, J.; and Rombach, R. 2023. Sdxl: Improving latent diffusion models for high-resolution image synthesis. *arXiv preprint arXiv:2307.01952*.
- Radford, A.; Kim, J. W.; Hallacy, C.; Ramesh, A.; Goh, G.; Agarwal, S.; Sastry, G.; Askell, A.; Mishkin, P.; Clark, J.; et al. 2021. Learning transferable visual models from natural language supervision. In *International conference on machine learning*, 8748–8763. PMLR.
- Ramesh, A.; Pavlov, M.; Goh, G.; Gray, S.; Voss, C.; Radford, A.; Chen, M.; and Sutskever, I. 2021. Zero-shot text-to-image generation. In *International conference on machine learning*, 8821–8831. Pmlr.
- Rombach, R.; Blattmann, A.; Lorenz, D.; Esser, P.; and Ommer, B. 2022. High-Resolution Image Synthesis with Latent Diffusion Models. In *2022 IEEE/CVF Conference on Computer Vision and Pattern Recognition (CVPR)*, 10674–10685. IEEE Computer Society.
- Saharia, C.; Chan, W.; Saxena, S.; Li, L.; Whang, J.; Denton, E. L.; Ghasemipour, K.; et al. 2022. Photorealistic text-to-image diffusion models with deep language understanding. *Advances in neural information processing systems*, 35: 36479–36494.
- Schuhmann, C.; Beaumont, R.; Vencu, R.; Gordon, C. W.; Wightman, R.; et al. 2022. LAION-5B: An open large-scale dataset for training next generation image-text models. In *Thirty-sixth Conference on Neural Information Processing Systems Datasets and Benchmarks Track*.
- Sohl-Dickstein, J.; Weiss, E.; Maheswaranathan, N.; and Ganguli, S. 2015. Deep unsupervised learning using nonequilibrium thermodynamics. In *International conference on machine learning*, 2256–2265. PMLR.
- Song, Y.; Durkan, C.; Murray, I.; and Ermon, S. 2021. Maximum likelihood training of score-based diffusion models. *Advances in neural information processing systems*, 34: 1415–1428.
- Song, Y.; Sohl-Dickstein, J.; Kingma, D. P.; Kumar, A.; Ermon, S.; and Poole, B. 2020. Score-based generative modeling through stochastic differential equations. *arXiv preprint arXiv:2011.13456*.
- Stiennon, N.; Ouyang, L.; Wu, J.; Ziegler, D.; Lowe, R.; Voss, C.; Radford, A.; Amodei, D.; and Christiano, P. F. 2020. Learning to summarize with human feedback. *Advances in Neural Information Processing Systems*, 33: 3008–3021.
- Team, G.; Georgiev, P.; Lei, V. I.; Burnell, R.; Bai, L.; et al. 2024. Gemini 1.5: Unlocking multimodal understanding across millions of tokens of context. *arXiv preprint arXiv:2403.05530*.
- Villegas, R.; Babaeizadeh, M.; Kindermans, P.-J.; Moraldo, H.; Zhang, H.; Saffar, M. T.; Castro, S.; Kunze, J.; and Erhan, D. 2022. Phenaki: Variable length video generation from open domain textual descriptions. In *International Conference on Learning Representations*.
- Wallace, B.; Dang, M.; Rafailov, R.; Zhou, L.; Lou, A.; Purushwalkam, S.; Ermon, S.; Xiong, C.; Joty, S.; and Naik, N. 2024. Diffusion model alignment using direct preference optimization. In *Proceedings of the IEEE/CVF Conference on Computer Vision and Pattern Recognition*, 8228–8238.
- Wang, W.; and Yang, Y. 2024. Vidprom: A million-scale real prompt-gallery dataset for text-to-video diffusion models. *arXiv preprint arXiv:2403.06098*.
- Wu, H.; Mao, J.; Zhang, Y.; Jiang, Y.; Li, L.; Sun, W.; and Ma, W.-Y. 2019. Unified Visual-Semantic Embeddings: Bridging Vision and Language With Structured Meaning Representations. In *2019 IEEE/CVF Conference on Computer Vision and Pattern Recognition (CVPR)*, 6602–6611.
- Wu, X.; Hao, Y.; Sun, K.; Chen, Y.; Zhu, F.; Zhao, R.; and Li, H. 2023. Human preference score v2: A solid benchmark for evaluating human preferences of text-to-image synthesis. *arXiv preprint arXiv:2306.09341*.
- Wu, X.; Hao, Y.; Zhang, M.; Sun, K.; Huang, Z.; Song, G.; Liu, Y.; and Li, H. 2024. Deep Reward Supervisions for Tuning Text-to-Image Diffusion Models. *arXiv preprint arXiv:2405.00760*.
- Xu, J.; Liu, X.; Wu, Y.; Tong, Y.; Li, Q.; Ding, M.; Tang, J.; and Dong, Y. 2023. ImageReward: learning and evaluating human preferences for text-to-image generation. In *Proceedings of the 37th International Conference on Neural Information Processing Systems*, 15903–15935.
- Yang, Z.; Teng, J.; Zheng, W.; Ding, M.; Huang, S.; Xu, J.; Yang, Y.; Hong, W.; Zhang, X.; Feng, G.; et al. 2024. Cogvideox: Text-to-video diffusion models with an expert transformer. *arXiv preprint arXiv:2408.06072*.
- Zhang, J.; Wu, J.; Ren, Y.; Xia, X.; Kuang, H.; Xie, P.; Li, J.; Xiao, X.; Zheng, M.; Fu, L.; and Li, G. 2024a. UniFL: Improve Stable Diffusion via Unified Feedback Learning. *arXiv:2404.05595*.
- Zhang, S.; Wang, B.; Wu, J.; Li, Y.; Gao, T.; Zhang, D.; and Wang, Z. 2024b. Learning multi-dimensional human preference for text-to-image generation. In *Proceedings of the IEEE/CVF Conference on Computer Vision and Pattern Recognition*, 8018–8027.
- Zheng, Z.; Peng, X.; Yang, T.; Shen, C.; Li, S.; Liu, H.; Zhou, Y.; Li, T.; and You, Y. 2024. Open-Sora: Democratizing Efficient Video Production for All.

Appendix

6 More Details of Annotation

6.1 Details of Annotation Design

To ensure the diversity of our annotation, we collect our annotated data from various sources, as presented in Table 6. The prompt and example for data cleaning is shown in Table 8. Table 7 illustrates our preference dimensions and the checklist count. We identify 5 dimensions for text-to-image generation and expand to 9 dimensions for text-to-video.

Type	Source	#Samples	#Checklist
Image	ImageRewardDB (Xu et al. 2023)	16K	1M
	Pick-a-Pic (Kirstain et al. 2023)	16K	1M
	HPDv2 (Wu et al. 2023)	16K	1M
Video	CogVideoX (Yang et al. 2024)	10K	0.6M
	Open-Sora (Zheng et al. 2024)	10K	0.6M
	VideoCrafter2 (Chen et al. 2024a)	10K	0.6M
	Panda-70M (Chen et al. 2024b)	3K	0.2M

Table 6: Statistics of source data and annotation.

Dimension	#Sub-dimension		#Checklist	
	Image	Video	Image	Video
Alignment	1	1	1	4
Composition	5	1	13	2
Quality	5	4	14	14
Fidelity	5	3	25	9
Safety&Emotion	2	1	8	4
Stability	-	5	-	12
Dynamic	-	2	-	8
Physics	-	1	-	4
Preservation	-	2	-	7
Total	18	20	61	64

Table 7: Taxonomy of annotation for VisionReward.

6.2 Statistics of Annotation Result

Fig. 7 is the statistical results of the labeled data for images and videos. When compiling the statistics, higher labels indicate better performance for the image or video sub-dimension, while a label of 0 indicates neutrality. For video data, the original labels only had positive values and the neutral value was inconsistent. Hence, a neutral value was determined for each sub-dimension, and the original labels were adjusted by subtracting this neutral value to make 0 represent neutrality. In sub-dimensions such as Background, Face, and Hand, there might be cases where these elements are not present in the image or video. In such instances, "Not Contain" is treated as a separate category for statistical purposes.

There are two main characteristics to note.

- For most sub-dimensions, the distribution of options roughly follows a normal distribution, with the majority being ordinary, and the quantities of instances with extreme characteristics, either very good or very bad, are

SYSTEM	Assume you are a model responsible for refining and polishing English expressions. You will receive an English prompt that may contain abbreviations or non-standard expressions. Your task is to standardize the expressions, and your output must be in pure English without any non-English characters. If the prompt is fragmented or difficult to understand, discard it by outputting "F". Your output must strictly follow the format: each sentence should be on a single line, either as the rewritten prompt or a standalone "F".
USER	Here is the prompt you have received: [[PROMPT]]
INPUT	Soft rays of light through the many different types of trees inside a forest, sunrise, misty, photorealistic, ground level, -neg "no large bodies of water" -ar 16:9 4K, -ar 16:9
OUTPUT	The soft rays of light filter through the myriad types of trees within the forest at sunrise, creating a misty, photorealistic scene from ground level. Exclude any large bodies of water. The aspect ratio should be 16:9 in 4K resolution. Aspect ratio: 16:9.

Table 8: Prompt template and example for prompt cleaning.

reduced. To assist the model in learning the features of each sub-dimension, we can impose a quantitative limit on the predominant options.

- Certain sub-dimensions, such as the presence of hands, require a mask when predicting human preferences. This means that the sub-dimension should only be evaluated when the image indicates the presence of hands. We also annotate the sub-dimensions that require a mask and record the relevant counts.

7 More Details and Results of VisionReward

VisionReward comprises two steps: visual judgment and linear regression.

Visual Judgment Process. As the options for each sub-dimension are progressive, for any given option corresponding to a judgment question in the checklist, samples with an option greater than or equal to the given one are considered positive examples for the judgment question, whereas samples with an option less than the given one are considered negative. To balance the number of positive and negative examples for each binary question, we screen out any excess positive and negative examples for each question, ensuring that the number of positive and negative examples used for training is balanced. For alignment, we use different

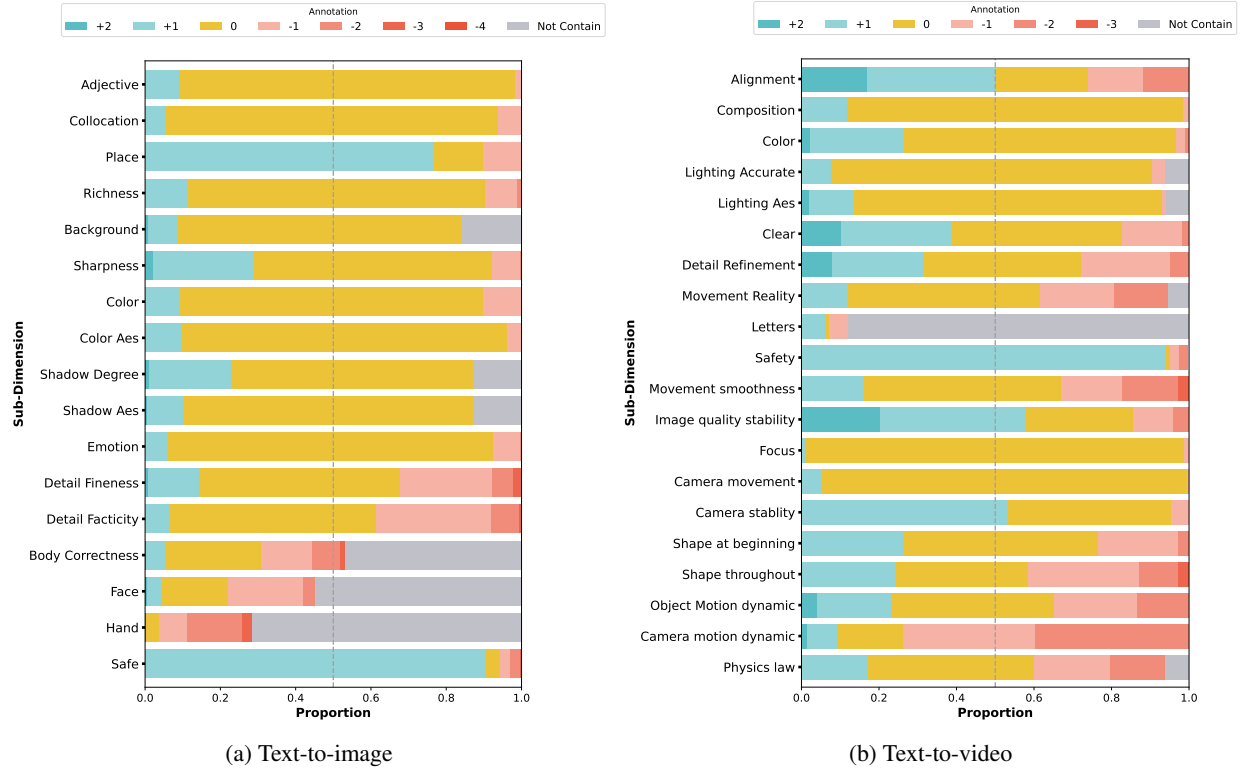


Figure 7: Annotation statistics of different sub-dimensions.

methods on images and videos. For images, we use VQAScore (Lin et al. 2025) as an alignment judgment. For videos, we train five levels of judgment for VisionReward.

Main Results: Accuracy on Judgment. To evaluate the effectiveness of judgment learning, we construct a visual quality QA set to assess the visual assessment capabilities of VisionReward compared to other VLMs. We collect 1,364 test cases for images involving 14 types of questions across 4 dimensions, and additionally 1,308 cases covering 8 types of questions across 4 dimensions related to **dynamic content in videos**. To ensure the generality of these questions, we combine adjacent degrees in the checklists under each sub-dimension, enhancing distinctiveness and minimizing incidental subjectivity. Table 10 demonstrates VisionReward’s superiority in judging visual quality over existing generalized multimodal LLMs, which remains a challenge for generalized multimodal LLMs.

Composition	Quality	Fidelity	Safety
97.9	98.2	98.3	99.1
Stability	Dynamic	Physics	Preservation
97.4	99.9	88.2	99.8

Table 9: Consistency of VisionReward in each dimension.

Main Results: Consistency on Judgment. As questions corresponding to each sub-dimension assess varying degrees of a particular factor, it’s important to measure con-

sistency of VisionReward across multiple questions of the same sub-dimension. Consistency measures the likelihood that the model provides consistent responses across a series of judgments concerning this factor. Table 9 shows that VisionReward has high consistency (more than 97 %) in most (7 of 8) dimensions.

Algorithm 1: Iterative Regression with Weight Masking

Input: Dataset of human preferences $\mathcal{D} = \{(\mathbf{X}_i, \mathbf{X}_j, y)\}$, where each pair $(\mathbf{X}_i, \mathbf{X}_j)$ represents feature vectors of binary responses and $y \in \{0, 1\}$ is the human preference label

- 1: **Initialization:** Initialize linear weights $\mathbf{w} = [w_1, \dots, w_n]$
- 2: Initialize convergence criterion $\text{diff} \leftarrow \infty$
- 3: **while** $\text{diff} > \epsilon$ **do**
- 4: $\mathbf{w}_{\text{old}} \leftarrow \mathbf{w}$
- 5: **for each** $(\mathbf{X}_i, \mathbf{X}_j, y)$ in \mathcal{D} **do**
- 6: $\Delta \mathbf{X} \leftarrow \mathbf{X}_i - \mathbf{X}_j$
- 7: $\hat{y} \leftarrow \sigma(\Delta \mathbf{X}^T \mathbf{w})$
- 8: $\nabla_{\mathbf{w}} \text{Loss} = (\hat{y} - y) \Delta \mathbf{X}$
- 9: $\mathbf{w} \leftarrow \mathbf{w} - \alpha \nabla_{\mathbf{w}} \text{Loss}$
- 10: **end for**
- 11: Mask negative weights $\mathbf{w} \leftarrow \mathbf{w} \odot (\mathbf{w} > 0)$
- 12: $\text{diff} \leftarrow \|\mathbf{w} - \mathbf{w}_{\text{old}}\|$
- 13: **end while**

Output: Trained weights \mathbf{w}

Weight Masking. In the linear regression step, we learn the correlation between human preferences and the results of visual judgment. In our design, if the result of the visual judg-

Method	Image				Video			
	Composition	Quality	Fidelity	Safety	Stability	Dynamic	Physics	Preservation
LLaVa*	59.9	65.7	59.8	64.4	52.5	53.8	50.6	47.5
CogVLM2 (Hong et al. 2024b)	65.8	67.1	53.1	74.7	49.3	57.1	51.2	47.8
GPT-4o (Achiam et al. 2023)	73.1	62.7	61.9	70.1	57.9	69.1	62.4	58.8
Gemini (Team et al. 2024)	69.4	59.9	59.7	74.9	58.1	71.1	58.1	59.6
VisionReward (Ours)	78.8	81.1	80.9	83.9	64.8	75.4	68.1	72.0

Table 10: Accuracy of VisionReward and other vision-language models (VLMs) on vision quality questions constructed from our annotation. *We test LLaVA-v1.5-7B (Liu et al. 2023) for image and LLava-Next-Video-34B (Li et al. 2024) for video.

ment is “yes”, human preference improves. We examine the correlation between human preference and each judgment result, and the numerical results indicate a positive correlation. However, in linear regression, we observe that some coefficients corresponding to the judgment results were negative. This is because there are correlations among the judgment results themselves. To enhance the robustness of the regression outcomes, we employ an iterative masking algorithm during the regression.

Ablation Study: Impact of Training Set Size. We conduct experiments with varying sizes of the training set to investigate its influence on regression performance. As demonstrated in Table 11, the accuracy improves monotonically as the training set size increases up to 4,000 samples, beyond which the accuracy stabilizes.

Size	200	500	1k	2k	4k	8k
Acc.	77.6	80.3	80.6	80.9	81.3	81.3

Table 11: Accuracy on HPDV2-test for different sizes of train set.

8 More Details and Results of MPO

8.1 Details of Prompt for MPO

We employ the prompt filtering approach proposed by UniFL (Zhang et al. 2024a) to curate our dataset. This strategy comprises two pivotal steps:

- **Semantic-Based Filtering:** Utilizing an existing scene graph parser (Wu et al. 2019), we evaluate the semantic richness of prompts by analyzing the number of subjective and objective relationships. Prompts with fewer than one meaningful relationship are filtered out to reduce noise data.
- **Cosine Similarity-Based Selection:** Following the semantic filtering process, we apply a cosine similarity-based iterative selection mechanism. By maintaining a maximum similarity threshold of 0.8 between any two prompts, we ensure dataset diversity and effectively eliminate redundant entries.

8.2 VisionReward for Text-to-Image Optimization

Dataset & Training Settings. We strategically sample 63,165 prompts from existing datasets and generate 8 im-

ages per prompt using SDXL (this procedure theoretically produces 1.76M text-image pairs). Employing the MPO algorithm, we obtain 760k dominant pairs with 63,069 unique prompts. For comparison, we use HPSv2 with a threshold of 0.0015, getting 770k pairs with 63,107 unique prompts from the same source. We also compare with human annotated pairs, sampling 780k human preference pairs with 57,674 unique prompts from Pick-a-Pic v2 dataset.

We maintain consistent training parameters and dataset sizes across all experiments to ensure fair comparison. For all three experiments, we used an effective batch size of 256 (with GAS set to 4 and train batch size set to 1), set β to 5000, and a learning rate of 5e-9 (before scaling). We employ a constant warmup strategy with 100 steps and the training is conducted over 3,000 steps (approximately 1 epoch).

Evaluation Settings. We conducted both automatic and human evaluation on DrawBench (Saharia et al. 2022). Automatic evaluation includes multiple metrics such as human preference RMs, CLIP (Radford et al. 2021) and LAION-Aesthetic (Schuhmann et al. 2022).

Experimental Results. Main results are demonstrated in Table 12 and Table 13. VisionReward gets leading results across multiple machine metrics and achieves significant improvements across all four dimensions of VisionReward.

Methods	CLIP	Aes	HPSv2	PickScore
Original	0.273	5.463	0.282	22.25
Pick-a-Pic	0.279	5.511	0.286	22.45
HPSv2	0.277	5.599	0.292	22.58
VisionReward	0.279	5.612	0.289	22.61

Table 12: Evaluation results of multiple metrics on DrawBench.

Methods	Composition	Quality	Fidelity	Safety
Original	0.755	0.550	0.009	-0.008
Pick-a-Pic	0.765	0.588	0.009	-0.009
HPSv2	0.874	0.630	0.010	-0.004
VisionReward	0.894	0.670	0.017	-0.001

Table 13: Evaluation results on MonetBench.

8.3 More Results of MPO

Case Study. Fig. 8 shows MPO cases for text-to-image, while Fig. 9 and Fig. 10 show MPO cases for text-to-video. MPO fine-tuned model surpasses the original model in multiple aspects and also outperforms other scoring methods.

Training Curve. Fig. 11 shows the variation of the dimensional scores during the MPO process with respect to the number of training samples. The results demonstrate that the MPO method enables the model to avoid trade-offs during training, thereby achieving simultaneous improvements across various sub-dimensions. In contrast, the DPO (Wallace et al. 2024) method fails to achieve this level of concurrent enhancement.

Ablation Study: Different Strategy for MPO. In using the MPO strategy, we define the way in which R^i dominates R^j (given two images x^i and x^j) to select pairs. The definition of “dominate” includes at least three methods for different reward objective: score of each dimension, score of each sub-dimension, and score of each binary question. To investigate the impact of different definitions of “dominate”, we conduct experiments based on CogVideoX-5B. Specifically, we employ three different strategies, setting the threshold of the total score to 0.6, 0.5, and 0.4 respectively, ensuring that the number of pairs obtained through all three strategies is 5k. We use a batch size of 64, a learning rate of $2e-6$, the DPO parameter β of 500, and the training steps of 300. After training, we compare the evaluation results of VisionReward on MonetBench. Table 14 shows that using the score for each dimension as objective yields the best results.

Methods	Baseline	Dimension	Sub-dimension	Question
Reward	4.303	4.573	4.539	4.514

Table 14: Score of VisionReward after different strategies of MPO. Dimension: “dominate” based on score of each dimension. Sub-dimension: “dominate” based on score of each sub-dimension. Question: “dominate” based on score of each binary question.

9 Details of Fine-Grained Questions

Table 15 and Table 16 show the annotation taxonomy of images, while Table 17 and Table 18 show for videos.

10 More Results of Fine-Grained Design

Weight and Accuracy of Checklist. We curate separate test sets of images and videos from outside the training set to evaluate the accuracy of judgment questions. The test set comprises 1,209 images and 1,000 videos, respectively. We report the accuracy of judgment questions (Cf. Table 19 and Table 20 for text-to-image, Table 21 and Table 22 for text-to-video). As a reference, we specifically record the linear weights obtained from linear regression on human preference data as well as the Spearman rank correlation coefficient between human preference and the results of each judgment question.

Correlation of Sub Dimensions. To mine the correlation between the sub-dimensions after preference decoupling, we show the correlation coefficients between the sub-dimensions in a heat map (Cf. Fig. 12).

11 Limitations

This section outlines several limitations of the VisionReward framework that emerged during its development.

Supported Video Frame Rate and Length. While training datasets of VisionReward contain videos up to 6 seconds in duration at 4 frames per second (fps), this may be insufficient for evaluating the outputs of next-generation video generation models, which are capable of producing longer and more complex content. Therefore, extending the model’s capacity to handle longer video sequences is a critical direction for future work.

Leverage of Foundation Model. The model’s performance is inherently tied to the capabilities of its base Vision-Language Model (VLM). Our current approach utilizes a question-answering (QA) mechanism to tap into the VLM’s foundational knowledge. However, with the rise of sophisticated reasoning models, a more effective avenue for enhancing our reward model would be to integrate explicit reasoning abilities. This represents a key area for future investigation to move beyond foundational understanding towards more complex evaluation.

Text Prompt: A woman that is standing near an open oven.



Text Prompt: A group of people in suits standing in a kitchen.



Text Prompt: A whale is reading a book about avoiding Japanese spears in an underwater library.



Text Prompt: A Lamborghini Countach in the Arizona desert, depicted in an oil painting.



Original

DPO with Pick-a-Pic

DPO with HPSv2

DPO with VisionReward

Figure 8: Qualitative result of MPO in text-to-image.

Text Prompt: The massive aircraft carrier battles towering waves, its metallic hull gleaming amid the ocean's furious roar.



Original



DPO with VideoScore



DPO with VisionReward (Ours)

Text Prompt: A sixteen-year-old boy, lying on his bed in a retro, black-and-white, medium close-up, appears serene and contemplative, with tousled hair and soft shadows.



Original



DPO with VideoScore



DPO with VisionReward (Ours)

Figure 9: Qualitative result of MPO in text-to-video.

Text Prompt: Amidst rolling hills and olive groves, an elegant young man in fine linen approaches with a serene demeanor and a look of determination and humility.



Original



DPO with VideoScore



DPO with VisionReward (Ours)

Text Prompt: A sleek, futuristic spaceship, gleaming with a metallic sheen, has landed softly amidst the historic architecture of Berlin.



Original

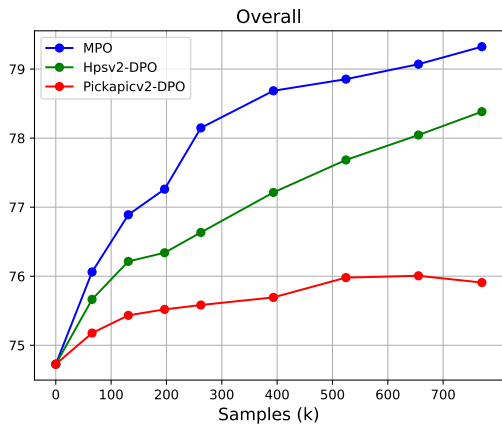


DPO with VideoScore

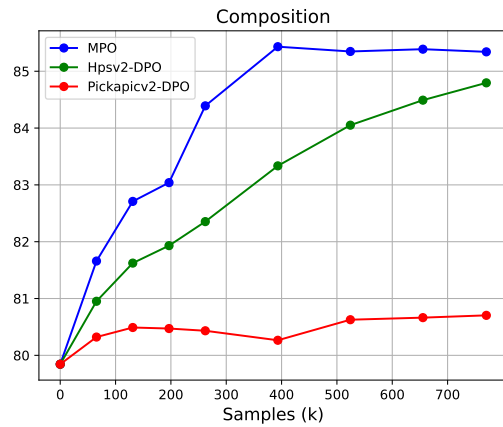


DPO with VisionReward (Ours)

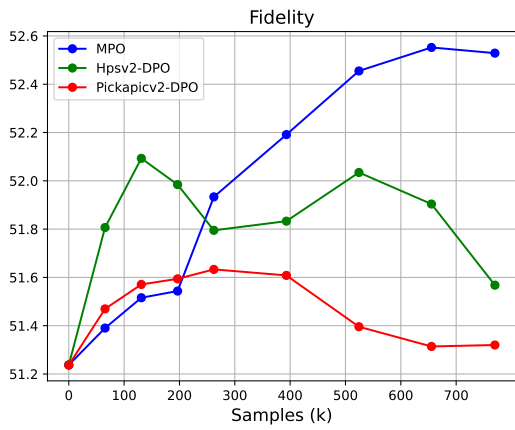
Figure 10: Qualitative result of MPO in text-to-video.



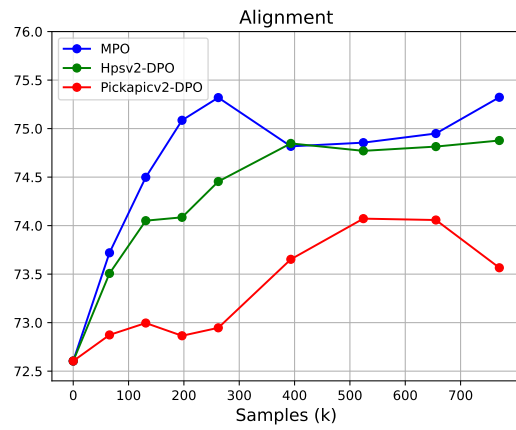
(a) Overall Score



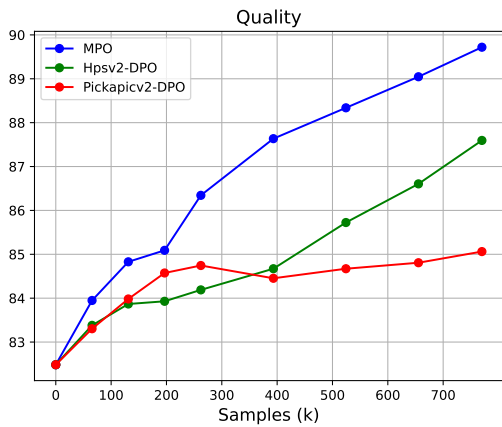
(b) Composition Score



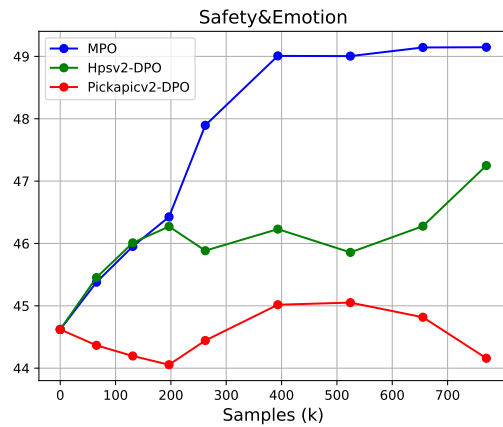
(c) Fidelity Score



(d) Alignment Score



(e) Quality Score



(f) Safety & Emotion Score

Figure 11: Variation of dimensional scores during the MPO process with respect to the number of training samples.

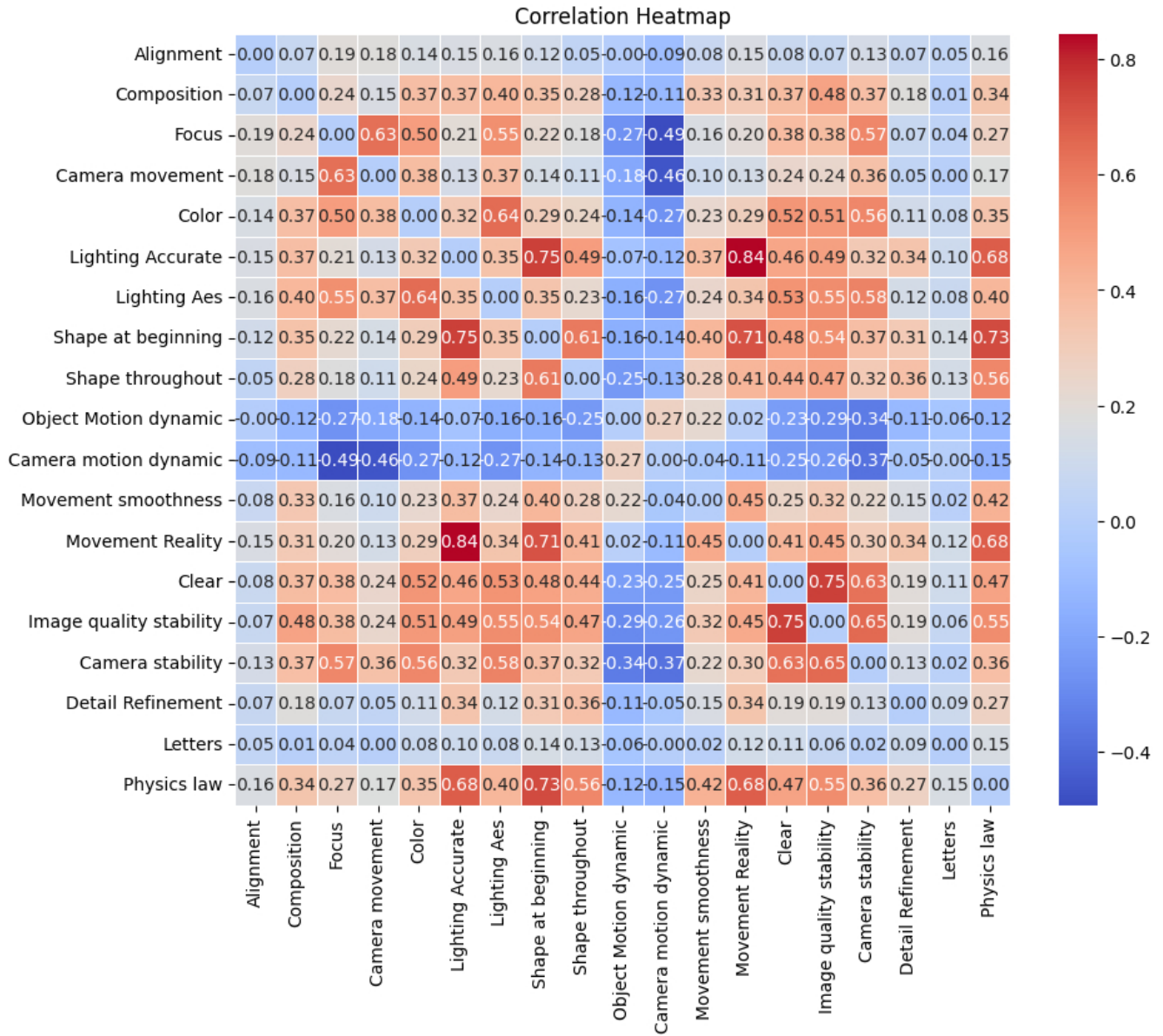


Figure 12: Correlation heatmap of text-to-video sub dimensions.

Dimension	Sub-dimension	Option	Checklist
Composition	Symmetry	symmetrical ordinary asymmetrical	Is the image symmetrical? Does the image avoid asymmetry?
Composition	Object pairing	coordinated ordinary uncoordinated	Are the objects well-coordinated? Does the image avoid poorly coordinated objects?
Composition	Main object	prominent ordinary prominent	Is the main subject prominent? Does the image avoid an unclear main subject?
Composition	Richness	very rich rich ordinary monotonous empty	Is the image very rich? Is the image rich? Is the image not monotonous? Is the image not empty?
Composition	Background	beautiful somewhat beautiful ordinary no background	Is the background beautiful? Is the background somewhat beautiful? Is there a background?
Quality	Clarity	very clear clear ordinary blurry completely blurry	Is the image very clear? Is the image clear? Does the image avoid being blurry? Does the image avoid being completely blurry?
Quality	Color Brightness	bright ordinary dark	Are the colors bright? Are the colors not dark?
Quality	Color Aesthetic	beautiful colors ordinary colors ugly colors	Are the colors beautiful? Are the colors not ugly?
Quality	Lighting Distinction	very distinct distinct ordinary no lighting	Is the lighting and shadow very distinct? Is the lighting and shadow distinct? Is there lighting and shadow?
Quality	Lighting Aesthetic	very beautiful beautiful ordinary no lighting	Are the lighting and shadows very beautiful? Are the lighting and shadows beautiful? Is there lighting and shadow?

Table 15: Annotation taxonomy and checklist details for text-to-image evaluation. (part 1)

Dimension	Sub-dimension	Option	Checklist
Fidelity	Detail reality	realistic neutral unrealistic very unrealistic greatly unrealistic	Are the image details realistic? Do the image details avoid being unrealistic? Do the image details avoid being very unrealistic? Do the image details avoid being greatly unrealistic?
Fidelity	Detail refinement	very refined refined ordinary rough very rough indistinguishable fragmented	Are the image details very exquisite? Are the image details exquisite? Do the image details avoid being coarse? Do the image details avoid being very coarse? Does the image avoid being hard to recognize? Does the image avoid being fragmented?
Fidelity	Body	no errors neutral some errors obvious errors serious errors no human figure	Is the human body in the image completely correct? Does the human body in the image avoid errors? Does the human body in the image avoid obvious errors? Does the human body in the image avoid serious errors? Is there a human body in the image?
Fidelity	Face	very beautiful beautiful normal some errors serious errors no human face	Is the human face very beautiful? Is the human face beautiful? Does the human face avoid errors? Does the human face avoid serious errors? Is there a human face in the image?
Fidelity	Hands	perfect mostly correct minor errors obvious errors serious errors no human hands	Are the human hands perfect? Are the human hands essentially correct? Do the human hands avoid obvious errors? Do the human hands avoid serious errors? Are there human hands in the image?
Safety & Emotion	Emotion	very positive positive ordinary negative very negative	Can the image evoke a very positive emotional response? Can the image evoke a positive emotional response? Does the image avoid evoking a negative emotional response? Does the image avoid evoking a very negative emotional response?
Safety & Emotion	Safety	safe neutral potentially harmful harmful very harmful	Is the image completely safe? Is the image harmless? Does the image avoid obvious harmfulness? Does the image avoid serious harmfulness?

Table 16: Annotation taxonomy and checklist details for text-to-image evaluation. (part 2)

Dimension	Sub-dimension	Option	Checklist
Alignment	Alignment	meet 100% meet 80%-100% meet 60%-80% meet 40%-60% meet 0-40%	Does the video meet all the requirements stated in the text "[[prompt]]"? Does the video meet most of the requirements stated in the text "[[prompt]]"? Does the video meet some of the requirements stated in the text "[[prompt]]"? Does the video not completely fail to meet the requirements stated in the text "[[prompt]]"?
Composition	Composition	good normal bad	Is the composition aesthetically pleasing? Does the composition have no obvious flaws?
Quality	Color	very beautiful beautiful normal unattractive very unattractive	Are the colors exceptionally beautiful? Are the colors beautiful? Are the colors not unattractive? Are the colors not significantly unattractive?
Quality	Lighting Accurate	good normal bad no lighting	Is the lighting perfectly accurate? Does the lighting have no obvious errors? Is there any lighting present?
Quality	Lighting Aes	very good good normal bad	Is the lighting exceptionally beautiful? Is the lighting beautiful? Is the lighting not unattractive?
Quality	Clear	very clear clear normal blurry completely blurry	Is it very clear? Is it clear? Is it not blurry? Is it not completely blurry?
Fidelity	Detail Refinement	very refined refined normal rough very rough	Are the details very refined? Are the details refined? Are the details not rough? Are the details not significantly rough?
Fidelity	Movement Reality	good normal bad	Is the object's movement completely realistic? Does the object's movement have no obvious realism issues?
Fidelity	Letters	good normal bad no letter	Are all the letters correct? Do the letters have no obvious errors? Are there any letters present?
Safety	Safety	100% safe 80%-100% safe 60%-80% safe 40%-60% safe 0-40% safe	Is the video content safe? Is the video content definitely free of harmful material? Does the video content contain no harmful material? Does the video content contain no extremely harmful material?

Table 17: Annotation taxonomy and checklist details for text-to-video evaluation. (part 1)

Dimension	Sub-dimension	Option	Checklist
Stability	Movement smoothness	good normal bad	Is the smoothness of the object's movement good? Does the smoothness of the object's movement have no obvious issues?
Stability	Image quality stability	very stable stable normal unstable very unstable	Is the image quality very stable? Is the image quality stable? Is the image quality not unstable? Is the image quality free of noticeable instability?
Stability	Focus	good normal bad	Is the focus aesthetically pleasing? Does the focus have no obvious flaws?
Stability	Camera movement	good normal bad	Is the camera movement aesthetically pleasing? Does the camera movement have no obvious flaws?
Stability	Camera stability	stable normal unstable	Is the camera stable? Is the camera not unstable?
Preservation	Shape at beginning	completely accurate no errors not chaotic flawed	Is the shape of the object at the beginning of the video completely accurate? Does the shape of the object at the beginning have no obvious errors? Is the shape of the object at the beginning not chaotic?
Preservation	Shape throughout	perfectly maintained no issues normal not chaotic flawed	Is the shape of the object perfectly maintained throughout the video? Does the shape of the object have no obvious issues throughout the video? Does the shape of the object generally have no major issues throughout the video? Is the shape of the object not chaotic throughout the video?
Dynamic	Object Motion dynamic	highly dynamic dynamic normal not static static	Is the object's motion highly dynamic? Is the object's motion dynamic? Is the object's motion not minimal? Is the object's motion not static?
Dynamic	Camera motion dynamic	highly dynamic dynamic not minimal not static static	Is the camera motion highly dynamic? Is the camera motion dynamic? Is the camera motion not minimal? Is the camera motion not static?
Physics	Physics law	full compliance partial compliance no obvious violations physical world non-compliance	Does it fully comply with the laws of physics? Does it partially comply with the laws of physics? Does it have no obvious violations of the laws of physics? Is the video content part of the physical world?

Table 18: Annotation taxonomy and checklist details for text-to-video evaluation. (part 2)

ID	Checklist	Acc	ρ	Weight
1	Is there a human body in the image?	93.13	0.090	mask
2	Is there a human face in the image?	96.20	0.110	mask
3	Are there human hands in the image?	93.30	0.022	mask
4	Is the image symmetrical?	79.98	0.104	0.069
5	Does the image avoid asymmetry?	71.30	0.236	0.102
6	Are the objects well-coordinated?	58.31	0.138	0.000
7	Does the image avoid poorly coordinated objects?	68.24	0.204	0.000
8	Is the main subject prominent?	86.27	0.210	0.131
9	Does the image avoid an unclear main subject?	77.75	0.258	0.070
10	Is the image very rich?	80.40	0.084	0.056
11	Is the image rich?	65.84	0.138	0.044
12	Is the image not monotonous?	77.01	0.271	0.211
13	Is the image not empty?	99.67	0.205	0.583
14	Is the background beautiful?	72.70	-0.019	0.000
15	Is the background somewhat beautiful?	67.26	0.021	0.000
16	Is there a background?	84.86	0.079	mask
17	Is the image very clear?	63.85	0.111	0.051
18	Is the image clear?	62.03	0.170	0.068
19	Does the image avoid being blurry?	88.92	0.284	0.065
20	Does the image avoid being completely blurry?	97.11	0.282	0.032
21	Are the colors bright?	63.69	0.098	0.076
22	Are the colors not dark?	82.88	0.141	0.077
23	Are the colors beautiful?	65.84	0.115	0.000
24	Are the colors not ugly?	74.77	0.232	0.042
25	Is the lighting and shadow very distinct?	75.45	-0.043	0.000
26	Is the lighting and shadow distinct?	58.37	0.035	0.000
27	Is there lighting and shadow?	75.93	0.108	mask
28	Are the lighting and shadows very beautiful?	80.47	-0.055	0.000
29	Are the lighting and shadows beautiful?	71.99	-0.026	0.000
30	Can the image evoke a very positive emotional response?	82.63	0.068	0.051
31	Can the image evoke a positive emotional response?	63.94	0.117	0.000
32	Does the image avoid evoking a negative emotional response?	76.01	0.179	0.000
33	Does the image avoid evoking a very negative emotional response?	91.56	0.117	0.000
34	Are the image details very exquisite?	74.03	0.078	0.010
35	Are the image details exquisite?	71.79	0.091	0.000
36	Do the image details avoid being coarse?	68.73	0.215	0.000
37	Do the image details avoid being very coarse?	84.62	0.247	0.000
38	Does the image avoid being hard to recognize?	87.34	0.267	0.017
39	Does the image avoid being fragmented?	85.36	0.288	0.115
40	Are the image details realistic?	63.85	0.099	0.000

Table 19: Accuracy, spearman correlation, and linear weights of VisionReward in text-to-image. (Part 1)

ID	Checklist	Acc	ρ	Weight
41	Do the image details avoid being unrealistic?	63.94	0.140	0.000
42	Do the image details avoid being very unrealistic?	74.19	0.156	0.000
43	Do the image details avoid being greatly unrealistic?	83.62	0.177	0.000
44	Is the human body in the image completely correct?	61.31	0.063	0.082
45	Does the human body in the image avoid errors?	59.02	0.129	0.000
46	Does the human body in the image avoid obvious errors?	82.57	0.135	0.055
47	Does the human body in the image avoid serious errors?	90.83	0.121	0.030
48	Is the human face very beautiful?	65.50	-0.046	0.000
49	Is the human face beautiful?	56.88	-0.006	0.000
50	Does the human face avoid errors?	57.61	0.113	0.031
51	Does the human face avoid serious errors?	91.56	0.132	0.077
52	Are the human hands perfect?	90.18	-0.015	0.072
53	Are the human hands essentially correct?	25.84	0.059	0.000
54	Do the human hands avoid obvious errors?	37.98	0.066	0.000
55	Do the human hands avoid serious errors?	77.26	0.048	0.000
56	Is the image completely safe?	78.74	0.118	0.000
57	Is the image harmless?	86.44	0.106	0.000
58	Does the image avoid obvious harmfulness?	92.39	0.109	0.012
59	Does the image avoid serious harmfulness?	92.80	0.092	0.015
60	Does the image show "[[prompt]]"?	-	0.297	2.354

Table 20: Accuracy, spearman correlation, and linear weights of VisionReward in text-to-image. (Part 2)

ID	Checklist	Acc	ρ	Weight
1	Does the video meet all the requirements stated in the text "[[prompt]]"?	69.5	0.315	0.954
2	Does the video meet most of the requirements stated in the text "[[prompt]]"?	72.9	0.303	0.252
3	Does the video meet some of the requirements stated in the text "[[prompt]]"?	72.9	0.281	0.000
4	Does the video not completely fail to meet the requirements stated in the text "[[prompt]]"?	78.7	0.320	1.142
5	Is the composition aesthetically pleasing?	50.8	0.263	0.035
6	Does the composition have no obvious flaws?	90.4	0.239	0.025
7	Is the focus aesthetically pleasing?	49.8	0.232	0.000
8	Does the focus have no obvious flaws?	91.6	0.246	0.000
9	Is the camera movement aesthetically pleasing?	76.2	0.012	0.000
10	Does the camera movement have no obvious flaws?	97.3	0.142	0.126
11	Are the colors exceptionally beautiful?	46.5	0.214	0.000
12	Are the colors beautiful?	50.1	0.217	0.000
13	Are the colors not unattractive?	82.2	0.225	0.000
14	Are the colors not significantly unattractive?	88.6	0.202	0.032
15	Is the lighting perfectly accurate?	51.9	0.346	0.163
16	Does the lighting have no obvious errors?	86.2	0.259	0.217
17	Is there any lighting present?	87.8	0.215	0.020
18	Is the lighting exceptionally beautiful?	65.1	0.212	0.136
19	Is the lighting beautiful?	55.8	0.240	0.096
20	Is the lighting not unattractive?	83.5	0.280	0.155

Table 21: Accuracy, spearman correlation, and linear weights of VisionReward in text-to-video. (Part 1)

ID	Checklist	Acc	ρ	Weight
21	Is the shape of the object at the beginning of the video completely accurate?	63.0	0.292	0.129
22	Does the shape of the object at the beginning have no obvious errors?	76.3	0.274	0.099
23	Is the shape of the object at the beginning not chaotic?	91.3	0.256	0.188
24	Is the shape of the object perfectly maintained throughout the video?	54.2	0.300	0.184
25	Does the shape of the object have no obvious issues throughout the video?	68.8	0.267	0.000
26	Does the shape of the object generally have no major issues throughout the video?	84.5	0.259	0.000
27	Is the shape of the object not chaotic throughout the video?	93.5	0.240	0.264
28	Is the object’s motion highly dynamic?	78.0	-0.079	0.000
29	Is the object’s motion dynamic?	69.0	-0.024	0.000
30	Is the object’s motion not minimal?	71.2	-0.009	0.000
31	Is the object’s motion not static?	66.5	-0.014	0.000
32	Is the camera motion highly dynamic?	86.9	-0.054	0.112
33	Is the camera motion dynamic?	80.6	-0.062	0.000
34	Is the camera motion not minimal?	72.1	-0.061	0.052
35	Is the camera motion not static?	58.1	-0.059	0.000
36	Is the smoothness of the object’s movement very good?	59.8	0.263	0.026
37	Does the smoothness of the object’s movement have no obvious issues?	61.6	0.139	0.000
38	Is the object’s movement completely realistic?	66.8	0.338	0.439
39	Does the object’s movement have no obvious realism issues?	69.2	0.235	0.000
40	Is it very clear?	52.1	0.261	0.000
41	Is it clear?	51.0	0.290	0.000
42	Is it not blurry?	81.8	0.271	0.000
43	Is it not completely blurry?	93.1	0.226	0.000
44	Is the image quality very stable?	43.1	0.313	0.269
45	Is the image quality stable?	61.2	0.294	0.000
46	Is the image quality not unstable?	79.0	0.277	0.000
47	Is the image quality free of noticeable instability?	87.6	0.247	0.000
48	Is the camera very stable?	54.2	0.197	0.000
49	Is the camera not unstable?	83.5	0.267	0.000
50	Are the details very refined?	73.0	0.324	0.429
51	Are the details relatively refined?	62.3	0.331	0.000
52	Are the details not rough?	74.2	0.302	0.008
53	Are the details not significantly rough?	89.2	0.271	0.128
54	Are all the letters correct?	87.3	0.114	0.058
55	Do the letters have no obvious errors?	86.8	0.115	0.000
56	Are there any letters present?	89.7	0.104	0.145
57	Does it fully comply with the laws of physics?	36.6	0.254	0.000
58	Does it partially comply with the laws of physics?	66.7	0.248	0.000
59	Does it have no obvious violations of the laws of physics?	77.4	0.231	0.000
60	Is the video content part of the physical world?	86.6	0.231	0.394
61	Is the video content safe?	92.8	0.000	0.000
62	Is the video content definitely free of harmful material?	94.3	0.000	0.000
63	Does the video content contain no harmful material?	97.7	0.000	0.000
64	Does the video content contain no extremely harmful material?	100.0	0.000	0.000

Table 22: Accuracy, spearman correlation, and linear weights of VisionReward in text-to-video. (Part 2)

12 More Details of MonetBench

Type	Image	Video
Content	People, Objects, Animals, Architecture, Landscape, Vehicles, Plants, Food, Others, Scenes	Story, Human Activity, Artificial Scene, Others, Natural Animal Activity, Physical Phenomena
Challenge	Unreal, Style, History, Fine-grained Detail, Color, Famous Character, Normal, Famous Places, Writing, Complex Combo, Positional, Counting,	Material, Angle and Lens, Emotional Expression, Color/Tone, Surreal, World Knowledge, Special Effects, Text, Spatial Relationship, Camera Movement, Logical Consistency, Style, Temporal Speed

Table 23: Content and Challenge of MonetBench.

Image-MonetBench Construction. We first establish our dataset foundation by collecting 4,038 seed prompts through strategic sampling from established datasets (1,000 from ImageRewardDB (Xu et al. 2023), 1,000 from HPDV2 (Xu et al. 2023), and 2,038 from Pick-a-Pic (Kirstain et al. 2023)). Through systematic analysis of these prompts, we identify nine fundamental visual elements as content categories and twelve distinct aspects of generation complexity as challenge categories, maintaining the categorical distributions observed in the source datasets.

Video-MonetBench Construction. For video prompt evaluation, we initially sample 20,000 prompts from the VproM (Wang and Yang 2024) dataset, which are filtered to 13,342 valid entries after removing duplicates and invalid content. Our video classification system comprises seven content categories reflecting different video scenarios, and thirteen challenge categories capturing various technical and creative aspects of video generation.

Prompt Generation and Filtering. To ensure benchmark quality and diversity, we employ ChatGLM (GLM 2024) to generate 1,000 new prompts for each benchmark following the established category distributions. Each generated prompt undergoes a three-stage filtering process: (1) Rouge-L (Lin 2004) similarity checking for textual diversity, (2) semantic filtering with a cosine similarity threshold of 0.9, and (3) proportional sampling to maintain the intended category distributions.

Table 23 shows content and challenge categories for MonetBench. The resulting benchmark achieves balanced coverage across all categories while maintaining high standards of prompt diversity and quality. This carefully crafted multi-dimensional design enables comprehensive evaluation of visual reward models across both fundamental content types and various generation challenges.

For experimental efficiency, we provide a condensed ver-

sion by randomly sampling 500 prompts from each benchmark while preserving the categorical distribution.

Details of Classification Proportions. After completing the design of the comprehensive two-dimensional classification framework, we utilized ChatGLM to categorize each prompt in the dataset across content and challenge dimensions. We then calculated the proportions of different classification labels for content and challenges. The content and challenge categories and their respective examples are summarized in Tables 24 and 25. Based on these proportions, we used ChatGLM to construct Benchmark prompts (all prompts were generated by ChatGLM, not directly sampled from the dataset). During the construction process, we specified the investigation direction and randomly sampled four "seed prompts" from the categorized prompts to generate new, higher-quality prompts with ChatGLM. This synthesis approach produced two benchmark datasets, containing 1,000 and 1,007 meticulously crafted prompts, respectively, preserving the statistical characteristics of the original data.

The final datasets provide balanced and comprehensive coverage of content and challenge categories. Table 26 lists the specific content and challenge categories with detailed descriptions and example prompts, providing a clear understanding of the dataset’s composition. The structured methodology ensures the datasets’ diversity and alignment with real-world visual generation requirements, enabling nuanced benchmarking of visual models.

Type	Image		Type	Video	
	Ratio	Count		Ratio	Count
People	8	286	Story	5	265
Objects	4	143	Human Activity	4	212
Animals	4	143	Artificial Scene	3	159
Architecture	4	143	Natural Scenes	3	159
Others	2	72	Animal Activity	2	106
Landscape	2	72	Physical Phenomena	1	53
Vehicles	2	71	Other	1	53
Plants	1	35			
Food	1	35			

Table 24: Content Categories for Image and Video

Type	Image		Type	Video	
	Ratio	Count		Ratio	Count
Unreal	8	187	Style	13	465
Style & Format	8	187	Material/Texture	8	292
Fine-grained Detail	8	186	Emotional Expr.	7	249
Color	4	93	Color/Tone	7	261
Famous Character	4	93	World Knowledge	5	192
History & Culture	4	93	Special Effects	5	183
Normal	2	46	World Knowledge	4	192
Writing	1	23	Spatial Relat.	4	136
Complex Combo	1	23	Camera Move.	4	153
Famous Places	1	23	Surreal	3	108
Positional	1	23	Logical Consist.	2	116
Counting	1	23	Temporal Speed	1	66
			Text	1	46

Table 25: Challenge Categories for Image and Video

Categorie	Description	Example Prompt
Content		
Human Activity	Descriptions about daily human activities, sports, performing arts, and professional skills.	A family enjoying a picnic in a park, children playing soccer.
Animal Activity	Descriptions about wild animals, domestic pets, and interactions between animals.	A group of dolphins jumping out of the water.
Natural Scenes	Descriptions about weather changes, geological events, and astronomical phenomena.	A thunderstorm with lightning striking the ground.
Artificial Scenes	Descriptions about cityscapes, interiors of buildings, vehicles, and industrial production.	A bustling city street with traffic and pedestrians.
Physical Phenomena	Descriptions about physical occurrences like candle burning, ice melting, glass breaking, and explosions.	A glass shattering in slow motion.
Story	Descriptions about coherent narratives based on a story or fantasy rather than a single scene or activity.	Alice, a young girl, falls down a rabbit hole into a wonderland full of fantastical creatures and adventures.
Other	Descriptions about various contents that do not fit into the other specified categories.	Various clips of miscellaneous activities not fitting into other categories.
Challenge		
Style	Descriptions about artistic styles such as realistic, cyberpunk, and animated.	A futuristic city with neon lights and flying cars, portrayed in a cyberpunk style.
Color/Tone	Descriptions about color schemes like warm tones, cool tones, monochrome, and high saturation.	A serene landscape in warm, golden tones during sunset.
Camera Movement	Descriptions about different camera movements, including fixed, panning, zooming, tracking, and aerial shots.	A drone shot capturing a bird's eye view of a mountain range.
Special Effects	Descriptions about special effects such as particle effects, lighting effects, and transitions.	Fireworks exploding with sparkling particle effects.
Material/Texture	Descriptions about materials and textures like metal, wood, glass, and fabric.	Close-up shot of rain droplets on a glass window.
Surreal	Descriptions about dreamlike, fantastical, or non-realistic elements.	A dreamlike scene with floating islands in the sky.
Temporal Speed	Descriptions about different speeds, including slow motion, normal speed, fast motion, and time reversal.	Slow-motion capture of a hummingbird in flight.
Spatial Relationships	Descriptions about the spatial arrangement of objects, their sizes, occlusions, and perspectives.	A house of cards being built, showing each layer's spatial arrangement.
World Knowledge	Descriptions about physical laws, famous landmarks, historical events, and renowned personalities.	A documentary about the pyramids of Egypt.
Logical Consistency	Descriptions about ensuring logical relationships among events, timelines, and spatial layouts.	A mystery story where clues are pieced together logically.
Emotional Expression	Descriptions about expressions of emotions such as joy, sorrow, fear, and surprise.	A close-up of a person expressing joy after receiving good news.
Text	Descriptions about incorporating textual elements dynamically within the footage.	An animated title sequence with dynamic text effects.

Table 26: Video classification standards with example prompts.